

## THE EFFECT OF GAS COOLING ON THE SHAPES OF DARK MATTER HALOS

STELIOS KAZANTZIDIS,<sup>1,2</sup> ANDREY V. KRAVTSOV,<sup>2</sup> ANDREW R. ZENTNER,<sup>2</sup> BRANDON ALLGOOD,<sup>3</sup>  
DAISUKE NAGAI,<sup>2</sup> AND BEN MOORE<sup>1</sup>

The Astrophysical Journal, accepted

### ABSTRACT

We analyze the effect of dissipation on the shapes of dark matter (DM) halos using high-resolution cosmological gasdynamics simulations of clusters and galaxies in the  $\Lambda$ CDM cosmology. We find that halos formed in simulations with gas cooling are significantly more spherical than corresponding halos formed in adiabatic simulations. Gas cooling results in an average increase of the principle axis ratios of halos by  $\sim 0.2-0.4$  in the inner regions. The systematic difference decreases slowly with radius but persists almost to the virial radius. We argue that the differences in simulations with and without cooling arise both during periods of quiescent evolution, when gas cools and condenses toward the center, and during major mergers. We perform a series of high-resolution  $N$ -body simulations to study the shapes of remnants in major mergers of DM halos and halos with embedded stellar disks. In the DM halo-only mergers, the shape of the remnants depends only on the orbital angular momentum of the encounter and not on the internal structure of the halos. However, significant shape changes in the DM distribution may result if stellar disks are included. In this case the shape of the DM halos is correlated with the morphology of the stellar remnants.

*Subject headings:* cosmology: theory — dark matter — galaxies: halos — halos: shapes — halos: structure — methods: numerical

### 1. INTRODUCTION

Triaxial dark matter (DM) halos are a generic prediction of the hierarchical, cold dark matter (CDM) model of structure formation. Therefore, observational probes of halo shapes are fundamental tests of this model. Recently, such comparisons have received attention as the accuracy and number of observational probes of halo shapes increase for the Milky Way (MW) (see Merrifield 2003, for a recent review), other galaxies (e.g., Buote & Canizares 1998; Buote et al. 2002; Hoekstra et al. 2004), and galaxy clusters (e.g., Kolokotronis et al. 2001).

Dubinski & Carlberg (1991) first pointed out that observed elliptical galaxies are systematically more spherical than simulated CDM halos. It was recently argued that the coherence of the tidal stream of the Sagittarius dwarf spheroidal galaxy indicates that the inner halo of the MW is nearly spherical, with a minor-to-major axis ratio  $c/a \gtrsim 0.8$  (Ibata et al. 2001; Majewski et al. 2003, but see Mayer et al. 2002, Helmi 2004, and Martínez-Delgado et al. 2004). This differs considerably from an average predicted ratio of  $\langle c/a \rangle \sim 0.6-0.7$  for MW-sized halos formed in *dissipationless* cosmological simulations (Barnes & Efstathiou 1987; Frenk et al. 1988; Dubinski & Carlberg 1991; Warren et al. 1992; Cole & Lacey 1996; Bullock 2002; Jing & Suto 2002). Although the axis ratios of simulated halos exhibit a broad distribution, with a Gaussian rms dispersion of  $\sim 0.1$ , we would have to accept the MW halo as an outlier.

Utilizing halo shapes as a test of the CDM paradigm requires improving both observations and theoretical predictions. Most of the numerical work published to date does not account for the effects of gas cooling on halo shapes. Notable exceptions are the studies by Katz & Gunn (1991), Evrard et al. (1994), and Tissera & Domínguez-Tenreiro (1998), who find that halos in dissipational simulations are systematically more spherical

than corresponding halos in dissipationless runs. However, the halos in these studies were resolved with only a few hundred to a few thousand particles and the shapes of the inner regions of halos could not be studied reliably. In addition, these studies did not address the processes by which cooling affects halo shapes. Recently, Floor et al. (2003) used gasdynamics simulations of galaxy clusters with and without radiative cooling to investigate the evolution of eccentricity. Their study showed very slow eccentricity evolution in simulated clusters. However, they focused on the eccentricity at large radii where, as we demonstrate, the effect of cooling is small.

Dubinski (1994) studied the effects of dissipation on halo shapes numerically by adiabatically growing central mass concentrations in an initially triaxial  $N$ -body halo. This study showed that the growth of a central condensation results in a considerably rounder halo shape. These experiments, although suggestive, were not generally representative of the cosmological framework of hierarchical halo assembly via multiple mergers.

In this Letter we revisit the effects of dissipation on halo shapes, combining self-consistent cosmological simulations with a resolution up to 2 orders of magnitude higher than in previous studies, with high-resolution controlled  $N$ -body simulations of binary mergers of disk galaxies and DM halos whose structure is based on the currently favored galaxy formation paradigm.

### 2. NUMERICAL SIMULATIONS

We analyze high-resolution cosmological simulations of eight group- and cluster-size systems and one galaxy-size system in a flat  $\Lambda$ CDM model:  $\Omega_m = 1 - \Omega_\Lambda = 0.3$ ,  $\Omega_b = 0.043$ ,  $h = 0.7$  and  $\sigma_8 = 0.9$ . The simulations were performed with the Adaptive Refinement Tree  $N$ -body+gasdynamics code (Kravtsov 1999; Kravtsov et al. 2002), an Eulerian code that uses adaptive refinement in space and time and (nonadaptive) refinement in mass to achieve the high dynamic range required to resolve cores of halos formed in cosmological simulations.

The cluster simulations have a peak resolution of  $\approx 2.44 h^{-1}$  kpc and DM particle mass of  $2.7 \times 10^8 h^{-1} M_\odot$  with only a region of  $\sim 10 h^{-1}$  Mpc around each cluster adaptively refined. We analyze each cluster at an epoch near  $z = 0$ , when it appears

<sup>1</sup> Institute for Theoretical Physics, University of Zürich, Winterthurerstrasse 190, CH-8057 Zürich, Switzerland; stelios@physik.unizh.ch.

<sup>2</sup> Department of Astronomy and Astrophysics, Kavli Institute for Cosmological Physics, 5640 South Ellis Avenue, University of Chicago, Chicago, IL 60637.

<sup>3</sup> Department of Physics, University of California at Santa Cruz, 1156 High Street, Santa Cruz, CA 95064.

most relaxed. This minimizes the noise introduced by substructure, which may cause transient changes in the estimates of axis ratios at particular radii. For one cluster, we also analyze its progenitors at  $z = 1$  and  $z = 2$ . The virial masses<sup>4</sup> of the clusters range from  $\approx 10^{13}$  to  $3 \times 10^{14} h^{-1} M_{\odot}$ . The galaxy formation simulation follows the early ( $z \geq 4$ ) evolution of a galaxy that becomes an MW-size object at  $z = 0$  in a periodic box of  $6 h^{-1}$  Mpc. At  $z = 4$ , the galaxy already contains a large fraction of its final mass:  $\approx 2 \times 10^{11} h^{-1} M_{\odot}$ . The DM particle mass is  $9.18 \times 10^5 h^{-1} M_{\odot}$  and the peak resolution of the simulation is  $183 h^{-1}$  comoving pc. This simulation is presented in Kravtsov (2003), where more details can be found.

For each object, we analyze two sets of simulations started from the same initial conditions but including different physical processes. The first set of simulations follows the dynamics of gas “adiabatically,” i.e., without radiative cooling. For the cluster halos we also analyze purely dissipationless simulations without gas the results of which agree well with the adiabatic gasdynamics runs. The second set of simulations includes star formation, metal enrichment and thermal supernovae feedback, metallicity- and density-dependent cooling, and UV heating due to a cosmological ionizing background. We use these cosmological simulations to study the effect of dissipation on the shapes of halos in the next section.

To explore the mechanisms responsible for the effect of cooling on halo shapes, we performed controlled  $N$ -body merger simulations of equal-mass pure DM halos and multicomponent galaxies varying only the internal mass distributions (Kazantzidis et al., in preparation). The DM halos followed the Navarro et al. (1996, hereafter NFW) density profile and were initially spherical with isotropic velocity dispersion tensors (Kazantzidis et al. 2004). First, we simulated several mergers of systems on parabolic orbits with pericenters that were 20% of the halo virial radii, typical of cosmological mergers (Khochfar & Burkert 2003). In one set of experiments, we merged DM halos with embedded stellar disks (Hernquist 1993; Mo et al. 1998). In these experiments we used randomly inclined and coplanar disk configurations and adopted halo parameters from the MW model A1 of Klypin et al. (2002). Specifically, each halo had a virial mass of  $M_{\text{vir}} = 7 \times 10^{11} h^{-1} M_{\odot}$ , a concentration parameter of  $c = 12$ , and a dimensionless spin parameter of  $\lambda = 0.031$ . The halos were adiabatically contracted to respond to the growth of the stellar disk. The mass and thickness of the stellar disk were  $M_d = 0.04 M_{\text{vir}}$  and  $z_0 = 0.1 R_d$ , respectively, and  $R_d = 2.7 h^{-1}$  kpc was the disk scale length. In another experiment, we studied the merging of identical NFW halos with no disk component. In a third experiment, we studied the merging of “contracted halos” with steepened inner density profiles ( $\rho \sim r^{-1.7}$ ). These profiles were set to match the combined initial spherical density profile of the adiabatically contracted halos and stellar disks in the halo+disk mergers. Last, we repeated the halo+disk and pure NFW halo mergers for radial orbits to study the effect of the impact parameter on the structure of the remnant (Moore et al. 2003). The initial separation of the halo centers was twice their virial radii. Their initial relative velocity was determined from the corresponding Keplerian orbit of two point masses for the parabolic mergers, while for the radial mergers it was set to the velocity of the circular orbit about their common center of mass.

The merger simulations were performed with the PKDGRAV

<sup>4</sup> We define the virial radius as the radius enclosing an average density of 180 times the mean density of the universe at the epoch of analysis.

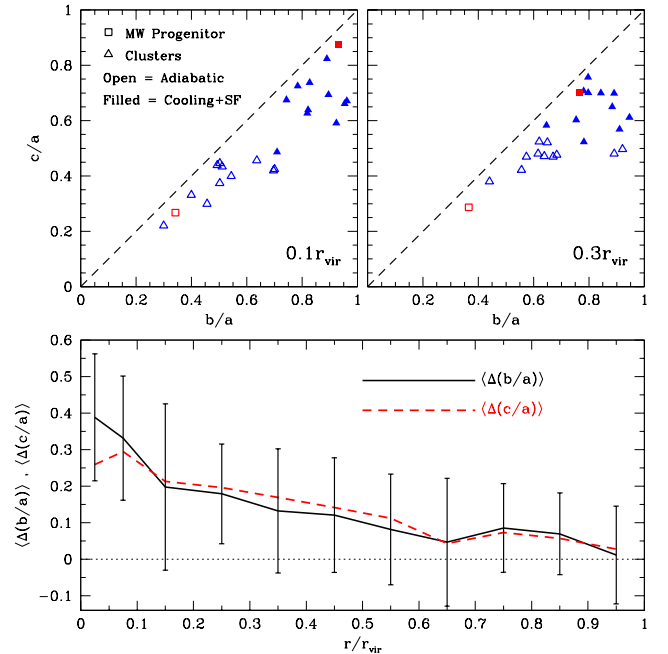


FIG. 1.— *Top panels:* Axis ratios  $c/a$  vs.  $b/a$  at 10% and 30% of the virial radius [using bins of  $\Delta(r/r_{\text{vir}}) = 0.1$ ] for halos in cosmological simulations. Open symbols show adiabatic simulations and filled symbols correspond to simulations with gas cooling and star formation. The galaxy simulation is shown by a square and the clusters by triangles. *Bottom panel:* Average difference between axis ratios in cooling and adiabatic simulations as a function of radius. The error bars show the  $1\sigma$  scatter about the mean value of  $\Delta(b/a)$  in each bin. The scatter in  $\Delta(c/a)$  is similar.

(Stadel 2001), multistepping, parallel  $N$ -body tree code. We used  $N = 2 \times 10^5$  DM particles and  $N = 2 \times 10^4$  collisionless stellar particles and employed a gravitational softening of 0.7 and  $0.3 h^{-1}$  kpc, respectively. Our results did not change when we used a factor of 10 more particles and half the softening indicating the achievement of numerical convergence.

### 3. RESULTS

For each object, we calculate principle axis ratios  $s = b/a$  and  $q = c/a$  ( $a > b > c$ ), from the eigenvalues of a modified inertia tensor (e.g., Dubinski & Carlberg 1991):  $I_{ij} = \sum_{\alpha} x_i^{\alpha} x_j^{\alpha} / r_{\alpha}^2$ , where  $x_i^{\alpha}$  is the  $i$  coordinate of the  $\alpha$ th particle,  $r_{\alpha}^2 = (y_1^{\alpha})^2 + (y_2^{\alpha}/s)^2 + (y_3^{\alpha}/q)^2$ , and  $y_i^{\alpha}$  are coordinates with respect to the principle axes. We use an iterative algorithm starting with a spherical configuration ( $a = b = c$ ) and use the results of the previous iteration to define the principle axes of the next iteration until the results converge to a fractional difference of  $10^{-3}$ . We compute axis ratios “differentially” using only particles within finite bins of  $r$ , and label each bin by the mean value of  $r$  of the particles in the bin. We use differential measurements because the axis ratios calculated at different values of  $r$  are almost independent. We find that in the standard practice of measuring shapes cumulatively and weighting each particle contribution to  $I_{ij}$  by  $r^{-2}$ , axis ratios at large  $r$  are quite sensitive to the distribution of particles in the inner regions of the halo. The differences between the differential and cumulative estimates of axis ratios can be as large as a few tenths at large radii. However, we present shape measurements in differential radial bins. Within each bin, different definitions of  $I_{ij}$  result in very small differences.

Figure 1 shows the principle axis ratios of the *dark matter* at

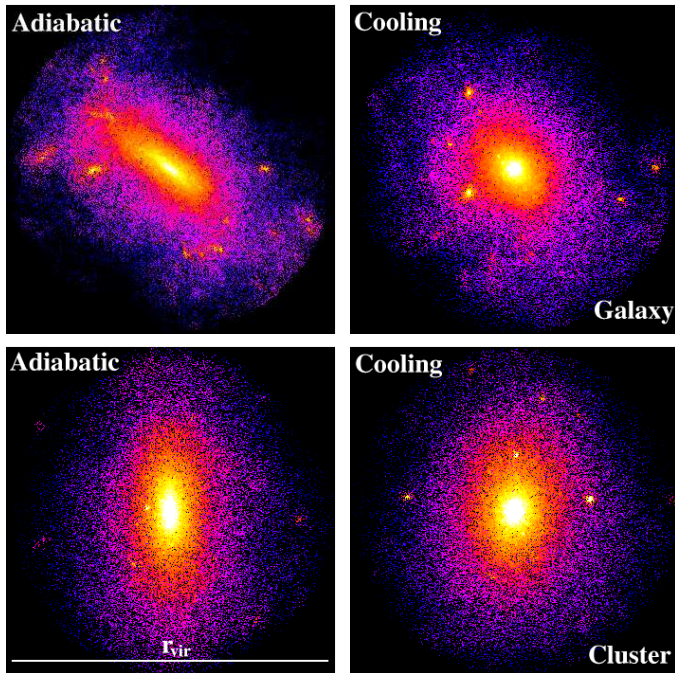


FIG. 2.— Density maps for the galaxy-size (*top panels*) and a cluster-size (*bottom panels*) halo projected onto the plane of intermediate and major axis. The particles are color-coded on a logarithmic scale with brighter colors in higher density regions. The local density is calculated using an SPH smoothing kernel of 64 particles to suppress small substructure and to better show the shape of the diffuse DM in the main halo. Halos in the cooling runs (*right panels*) are significantly rounder than their adiabatic counterparts (*left panels*).

10% and 30% of the virial radius for all cosmological simulations. The purely dissipationless simulations without gas produce results similar to the adiabatic runs and are omitted for clarity. Note that the halos in adiabatic simulations tend to be slightly more elongated closer to their centers. Interestingly, there is a correlation of  $c/a$  and  $b/a$ . The effect of cooling changes axis ratios roughly along the correlation in the  $c/a$ - $b/a$  plane by up to  $\sim 0.4$  at  $0.1r_{\text{vir}}$  and by  $\sim 0.2$ – $0.3$  at  $0.3r_{\text{vir}}$ . The significance of the change in shape can be seen in Figure 2, where we show density maps of the DM distribution in the simulated galaxy (*top panels*) and a cluster (*bottom panels*) at  $z=4$  and  $z=0.4$ , respectively. The difference between the adiabatic and cooling simulations is visually striking, with the DM halos significantly rounder in the cooling runs.

The radial dependence of the effect can be seen in the bottom panel of Figure 1, which shows the average difference between axis ratios in the cooling and adiabatic runs [ $\Delta(b/a) \equiv (b/a)_{\text{cool}} - (b/a)_{\text{adiab}}$ ] as a function of radius. Although the effect decreases with radius, the axis ratios in simulations with cooling are systematically larger than in the adiabatic and dissipationless cases, even at  $r \approx 0.8r_{\text{vir}}$ . Figure 3 shows individual radial profiles of the minor-to-major axis ratio  $c/a$  in the galaxy and cluster simulations, as well as in representative controlled merger experiments. It is interesting to compare cluster and galaxy halos because their baryon distributions have different morphologies. In the galaxy, most ( $\sim 90\%$ ) of the baryons lie in a highly flattened gaseous disk, while in the cluster simulations most of the baryons are in stars in a massive, central elliptical galaxy. For both the galaxy and the cluster systems the effect of cooling is only weakly dependent on radius and is significant even at  $r_{\text{vir}}$ . Note that axis ratios are not constant as a function of

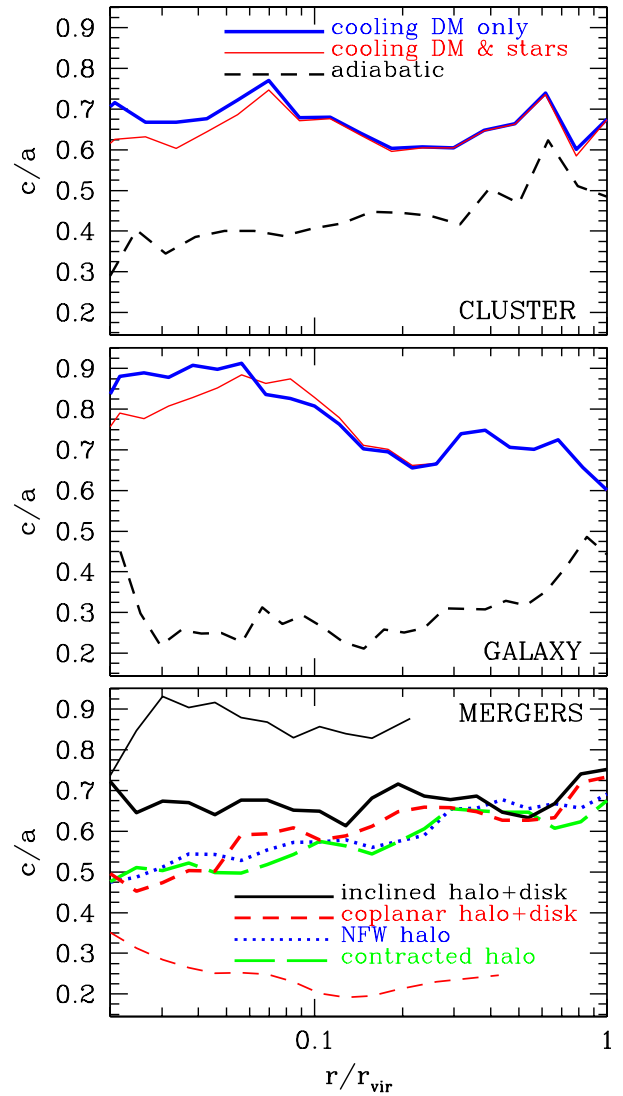


FIG. 3.— *Top and middle panels*: Minor-to-major axis ratio,  $c/a$ , as a function of radius for a cluster-size (*top panel*) and the galaxy-size (*middle panel*) halo. The thick solid lines correspond to the DM, while the thin solid lines show the combined  $c/a$  of DM and stars in simulations with cooling. The dashed lines show the profile of the DM in the adiabatic simulations. *Bottom panel*: The  $c/a$  profiles of merger remnants. We show remnants from four mergers: inclined halo+disk (*solid line*), coplanar halo+disk (*short-dashed line*), NFW halo (*dotted line*), and contracted halo (*long-dashed line*). Thick lines show  $c/a$  for DM only, and thin lines show  $c/a$  for stars in the cases with initial stellar disks in the inclined (*solid line*) and coplanar (*short-dashed line*) mergers. We show the profiles at a time  $\sim 8$  crossing times of the remnant.

radius and that changes are not monotonic. Different regions of an object may be flattened to different degrees. This indicates that observational estimates of halo shapes in the disk region (e.g., by disk flaring, Olling & Merrifield 2000) may be somewhat different from results at larger distances. Note that despite the significant flattening of the baryons in the central  $0.1r_{\text{vir}}$  of the galaxy simulation, the DM distribution around the disk is almost spherical.

It is interesting to ask if the ellipsoid of the DM halo is aligned with that of the baryons. For clusters, in which most of the baryons in the center are in stars, the major axes of the stellar and DM distribution are approximately aligned at all radii. For example, the major axis of the central cluster galaxy is well aligned with the inner DM halo. However, we find that in clus-

ters that contain massive substructures in their outer regions, the direction of the major axis often changes dramatically at  $r \gtrsim 0.5r_{\text{vir}}$ . In the galaxy simulation, the minor axis of the DM distribution in the vicinity of the disk is aligned with the minor axis of the disk. However, the flattening of the DM distribution is small (Figure 3). Interestingly, at  $r \gtrsim 0.2r_{\text{vir}}$ , the direction of the major axis of the DM halo changes and is nearly perpendicular to the disk.

We examined the evolution of the merger remnants and found that their shapes evolve in their outer regions for  $\sim 8$  crossing times or  $\sim 14\text{--}18$  Gyr. This indicates that the shapes of the outer regions of the cosmological halos are evolving at all epochs. The bottom panel of Figure 3 shows the axis ratios of the remnants in controlled merger experiments after 8 crossing times, when the evolution has ceased. The shapes of the DM halo merger remnants vary, depending strongly on the presence of a disk component and the relative inclination of disks prior to the merger. Mergers of halos with different central density profiles produce remnants with very similar axis ratios. When a disk component is present, the shape of the remnant DM halo depends sensitively on the initial relative inclination of the disks. Inclined disk mergers lead to a very spherical stellar remnant and a correspondingly more spherical DM halo, compared to the halo-only cases. Coplanar disk mergers lead to a very disklike stellar component (small  $c/a$ ) and a DM halo that is nearly as flattened as in the halo-only mergers. We discuss the implications of these results in the next section.

#### 4. DISCUSSION AND CONCLUSIONS

We show that halos in cosmological simulations with cooling are considerably more spherical than those in dissipationless simulations. The difference decreases with increasing radius but can be significant even at the virial radius. This is somewhat surprising because cooling affects the mass distribution appreciably only in the inner  $\sim 10\%$  of the virial radius. The condensation of baryons due to cooling leads to a more concentrated distribution of DM, as it responds to the increasing gravitational field of baryons in the center (Blumenthal et al. 1986). Thus, dissipation results in a significantly more centrally concentrated mass distribution and a deeper gravitational potential. Dubinski (1994) showed that this leads to the evolution of the halo toward a more spherical shape in a few crossing times, arguing that as the central condensation grows, the overall potential becomes rounder. This shifts the boundaries between orbital families markedly, decreasing the fraction of regular box orbits that serve as the backbone of a triaxial mass distribution (Gerhard & Binney 1985; Udry & Martinet 1994; Barnes & Hernquist 1996; Merritt & Quinlan 1998; Valluri & Merritt 1998).

In hierarchical models of structure formation, halos grow via a sequence of violent mergers and periods of slow accretion. Although cooling can gradually make a halo more spherical, subsequent mergers can produce highly elongated remnants (e.g., Moore et al. 2003), erasing the effect of dissipation discussed above. If no significant cooling occurs after the last major merger,<sup>5</sup> the triaxiality of the halo will be largely determined by the merger. Hence it is important to consider how cooling affects the shapes of merger remnants. To this end, we analyze a suite of controlled merger simulations of pure DM halos and halos with embedded disks.

<sup>5</sup> For example, if the merger occurs after most of the gas is converted to stars or the cooling time in the merger remnant is long.

Cooling can directly affect the shape of stellar remnants during mergers (Barnes & Hernquist 1996). However, a large amount of cooling gas may be needed for this to significantly affect the shapes of DM halos. Indeed, we compare remnant shapes in mergers of disk+halo systems in which disks contain both stars and a modest amount of gas (10% of the total disk mass), with and without cooling. This comparison shows that the effect of dissipation on the shapes of dark halos during the mergers of these stellar-dominated disks is negligible.

On the other hand, our merger simulations demonstrate that the shape of the remnant DM halo is affected by the presence of cold stellar disks. Figure 3 shows that the shape of the DM distribution in the remnant is always correlated with the shape of the stellar distribution. Inclined disk mergers produce a nearly spherical stellar remnant, while coplanar disk mergers yield a very oblate stellar remnant with  $c/a \sim 0.3$ . The corresponding DM distribution is also more spherical in the inclined disk merger. The shape of the stellar remnant is thus quite sensitive to the mutual orientation of the merging disks. It is likely to be also sensitive to their internal properties. Indeed, in an inclined halo+disk merger with the same orbital parameters as before, but with a factor of 3 thicker stellar disks, the stellar remnant is less spherical and the halo axis ratios are lower by  $\sim 0.15$  in the inner  $r \lesssim 0.1r_{\text{vir}}$ . If a spherical remnant is formed, the potential in the central region, where stars dominate gravitationally, will also be spherical. This likely destroys the regular box orbits of DM particles and drives the DM distribution to a more spherical configuration. This effect is not confined to the vicinity of the stellar remnant. The DM distribution may be affected at larger radii because DM particles in CDM halos are, on average, on eccentric orbits with a median apocenter-to-pericenter ratio of  $r_{\text{apo}}/r_{\text{per}} = 6/1$  (Ghigna et al. 1998).

Our results indicate that the effect of cooling during quiescent evolution and its indirect effect during late-time disk mergers are both important in determining the shape of the final mass distribution. These effects lead to halos that are systematically more spherical than those measured in dissipationless CDM simulations. This has several important implications for comparisons with, and interpretations of, observations. The mean axis ratios of MW-size halos may be expected to be  $\langle c/a \rangle \sim 0.7\text{--}0.8$  in their inner regions compared to  $\langle c/a \rangle \sim 0.6\text{--}0.7$  estimated from dissipationless  $N$ -body simulations. This can explain the observed coherence of the tidal streams of the Sagittarius dwarf spheroidal galaxy without requiring the MW halo to be an outlier in the distribution of halo shapes. We may also expect any intrinsic correlations between the shapes of neighboring galaxies to be mitigated. The effect of triaxiality on the average lensing cross section of clusters may not be as strong as previously thought (Dalal et al. 2003; Oguri & Keeton 2004). More spherical inner halos may influence the dynamics of bars and stars in galactic disks (e.g., El-Zant & Shlosman 2002; Gadotti & de Souza 2003) and may limit the mass of nuclear supermassive black holes by inhibiting their fueling (Merritt & Quinlan 1998).

The effect of cooling is likely to be mass dependent because the efficiency of cooling and star formation, manifested in the average mass-to-light ratio  $M/L$ , is a fairly strong non-monotonic function of mass (e.g., van den Bosch et al. 2003). Current cosmological simulations that include gasdynamics suffer from the ‘‘overcooling problem’’: the fraction of baryons in stars and cold gas is at least a factor of 2 higher than observed for the systems of the mass range that we consider (Lin et al. 2003).

The effect on the axis ratios is therefore likely overestimated and substantial improvements in cosmological simulations are required to predict the shape distribution of CDM halos accurately. Nevertheless, the effect that we find is so strong that even with significantly reduced fractions of cold gas, we expect the change in the axis ratios in the inner regions of halos to be  $\gtrsim 0.1$ , comparable to or larger than the dispersion in the distribution of measured axis ratios in dissipationless  $N$ -body simulations.

We thank Victor Debattista, John Dubinski, Lucio Mayer, and Monica Valluri for useful discussions. B. M. would like to thank John Magorrian for valuable comments on shape and orbital structure. S. K. is grateful to the Kavli Institute for Cosmological Physics at the University of Chicago for the hospitality during his visit. This work is supported by the NSF and NASA under grants AST 02-06216, AST 02-39759, NAG5-13274, and NAG5-7986 and by the Kavli Institute for Cosmological Physics at the University of Chicago and the Institute for Theoretical Physics at the University of Zürich. D. N. is supported by the NASA Graduate Student Researchers Program. The cosmological simulations used in this study were performed on the IBM RS/6000 SP4 system at the National Center for Supercomputing Applications. The merger simulations were carried out on the Intel cluster at the Cineca Supercomputing Center in Bologna, Italy.

## REFERENCES

- Barnes, J. & Efstathiou, G. 1987, *ApJ*, 319, 575  
 Barnes, J. E. & Hernquist, L. 1996, *ApJ*, 471, 115  
 Blumenthal, G. R., Faber, S. M., Flores, R., & Primack, J. R. 1986, *ApJ*, 301, 27  
 Bullock, J. S. 2002, in Proceedings of the Yale Cosmology Workshop "The Shapes of Galaxies and Their Dark Matter Halos", New Haven, Connecticut, USA, 28-30 May 2001. Priyamvada Natarajan, Ed.. Singapore: World Scientific, 2002, *astro-ph/0106380*, 109  
 Buote, D. A. & Canizares, C. R. 1998, in ASP Conf. Ser. 136: Galactic Halos, 289  
 Buote, D. A., Jeltema, T. E., Canizares, C. R., & Garmire, G. P. 2002, *ApJ*, 577, 183  
 Cole, S. & Lacey, C. 1996, *MNRAS*, 281, 716  
 Dalal, N., Holder, G., & Hennawi, J. 2003, *ApJ* submitted (*astro-ph/0310306*)  
 Dubinski, J. 1994, *ApJ*, 431, 617  
 Dubinski, J. & Carlberg, R. G. 1991, *ApJ*, 378, 496  
 El-Zant, A. & Shlosman, I. 2002, *ApJ*, 577, 626  
 Evrard, A. E., Summers, F. J., & Davis, M. 1994, *ApJ*, 422, 11  
 Floor, S., Melott, A., & Motl, a. P. 2003, *ApJ*, in press, (*astro-ph/0307539*)  
 Frenk, C. S., White, S. D. M., Davis, M., & Efstathiou, G. 1988, *ApJ*, 327, 507  
 Gadotti, D. A. & de Souza, R. E. 2003, *ApJ*, 583, L75  
 Gerhard, O. E. & Binney, J. 1985, *MNRAS*, 216, 467  
 Ghigna, S., Moore, B., Governato, F., Lake, G., Quinn, T., & Stadel, J. 1998, *MNRAS*, 300, 146  
 Helmi, A. 2004, *MNRAS*, in press (*astro-ph/0309579*)  
 Hernquist, L. 1993, *ApJS*, 86, 389  
 Hoekstra, H., Yee, H. K. C., & Gladders, M. D. 2004, *ApJ* in press, *astro-ph/0306515*  
 Ibata, R., Lewis, G. F., Irwin, M., Totten, E., & Quinn, T. 2001, *ApJ*, 551, 294  
 Jing, Y. P. & Suto, Y. 2002, *ApJ*, 574, 538  
 Katz, N. & Gunn, J. E. 1991, *ApJ*, 377, 365  
 Kazantzidis, S., Magorrian, J., & Moore, B. 2004, *ApJ*, 601, 37  
 Khochfar, S. & Burkert, A. 2003, *MNRAS* submitted (*astro-ph/0309611*)  
 Klypin, A., Zhao, H., & Somerville, R. S. 2002, *ApJ*, 573, 597  
 Kolokotronis, V., Basilakos, S., Plionis, M., & Georgantopoulos, I. 2001, *MNRAS*, 320, 49  
 Kravtsov, A. V. 1999, PhD thesis, New Mexico State University  
 —. 2003, *ApJ*, 590, L1  
 Kravtsov, A. V., Klypin, A., & Hoffman, Y. 2002, *ApJ*, 571, 563  
 Lin, Y., Mohr, J. J., & Stanford, S. A. 2003, *ApJ*, 591, 749  
 Majewski, S. R., Skrutskie, M. F., Weinberg, M. D., & Ostheimer, J. C. 2003, *ApJ*, 599, 1082  
 Martínez-Delgado, D., Gómez-Flechoso, M. Á., Aparicio, A., & Carrera, R. 2004, *ApJ*, 601, 242  
 Mayer, L., Moore, B., Quinn, T., Governato, F., & Stadel, J. 2002, *MNRAS*, 336, 119  
 Merrifield, M. R. 2003, in to be published in the proceedings of IAU Symposium 220 "Dark Matter in Galaxies," Sydney, July 2003, ASP Conf. Series, (*astro-ph/0310497*)  
 Merritt, D. & Quinlan, G. D. 1998, *ApJ*, 498, 625  
 Mo, H. J., Mao, S., & White, S. D. M. 1998, *MNRAS*, 295, 319  
 Moore, B., Kazantzidis, S., Diemand, J., & Stadel, J. 2003, *MNRAS* submitted, (*astro-ph/0310660*)  
 Navarro, J. F., Frenk, C. S., & White, S. D. M. 1996, *ApJ*, 462, 563  
 Oguri, M. & Keeton, C. R. 2004, *ApJ* submitted (*astro-ph/0403633*)  
 Olling, R. P. & Merrifield, M. R. 2000, *MNRAS*, 311, 361  
 Stadel, J. G. 2001, Ph.D. Thesis, Univ. of Washington  
 Tissera, P. B. & Domínguez-Tenreiro, R. 1998, *MNRAS*, 297, 177  
 Udry, S. & Martinet, L. 1994, *A&A*, 281, 314  
 Valluri, M. & Merritt, D. 1998, *ApJ*, 506, 686  
 van den Bosch, F. C., Yang, X., & Mo, H. J. 2003, *MNRAS*, 340, 771  
 Warren, M. S., Quinn, P. J., Salmon, J. K., & Zurek, W. H. 1992, *ApJ*, 399, 405